

Dioxovanadium(V) Complexes of Schiff and Tetrahydro-Schiff Bases Encapsulated in Zeolite-Y for the Aerobic Oxidation of Styrene¹

Zhongzhen Ding^a and Ying Yang^{b, *}

^aSchool of Material Science and Engineering, Tianjin Polytechnic University, Xiqing District, Tianjin 300387, China

^bState Key Laboratory of Heavy Oil Processing, China University of Petroleum, Changping, Beijing 102249, China

*e-mail: catalyticsscience@163.com

Received September 24, 2016

Abstract—A series of dioxovanadium(V) complexes of Schiff and tetrahydro-Schiff bases were encapsulated into the supercages of zeolite-Y and were characterized by X-ray diffraction, SEM, N₂ adsorption/desorption, FT-IR, UV-vis spectroscopy, ICPAES, pair distribution function (PDF) and X-ray absorption near edge structure (XANES) measurements. The encapsulation is achieved by a flexible ligand method in which the transition metal cations were first ion-exchanged into zeolite-Y and then complexed with ligands. The dioxovanadium-exchanged zeolite, dioxovanadium complexes encapsulated in zeolite-Y plus non-encapsulated homogeneous counterparts were all screened as catalysts for the aerobic oxidation of styrene under mild conditions. It was found that the encapsulated complexes showed better activity than their respective non-encapsulated counterparts in most cases. All encapsulated dioxovanadium tetrahydro-Schiff base complexes showed much higher activity in aerobic oxidation of styrene than their corresponding Schiff base complexes.

Keywords: dioxovanadium complexes, Schiff and tetrahydro-Schiff bases, zeolite-Y, XANES, catalytic activity, aerobic oxidation, styrene

DOI: 10.1134/S0023158417030053

1. INTRODUCTION

The oxidation of styrene is of great interest because styrene oxide and benzaldehyde are important and versatile synthetic intermediates in chemical industry [1, 2]. Currently, a wide range of homogeneous metal complexes for styrene oxidation exist, but most of them suffer from severe deactivation due to easy formation of dimeric peroxy- and μ -oxo species. Heterogenization of these homogeneous catalysts onto solid supports has been sought to isolate metal complexes to prevent their dimerization, increase their ruggedness and separability [3–8]. In this respect, encapsulation of transition metal complexes into zeolites gained much interest in the last decade, since not only the encapsulation strategy is found to be convenient and advantageous, because the metal complex, once formed inside pore cavity, is not easy to diffuse out and to enter the liquid phase during catalytic reaction, but also this process can give rise to the materials with both homogeneous and heterogeneous catalysis characters [9]. Faujasite zeolite including zeolite X and Y, is frequently chosen as support to encapsulate metal complexes because of its huge supercage (13 Å) with smaller pore opening (ca. 8 Å) suitable to accommodate metal complexes and three-dimensional pore sys-

tem desirable for easy reactant accessibility and product diffusion [10]. Metalloporphyrins and metallophthalocyanines are usually encapsulated into zeolite-Y for the oxidation of alkanes, alkenes, alcohols and so on. For example, Balkus and coworkers synthesized a NaX encapsulated ruthenium perfluorophthalocyanine complex (RuF₁₆Pc-X) and it proved to be efficient for the oxidation of cyclohexane with *tert*-butyl hydroperoxide as the oxidant [11].

Schiff base transition metal complexes have been extensively studied because of their potential use as catalysts in a wide range of oxidation reactions [12–15]. However, the number of encapsulated Schiff base complexes is very limited owing to the presence of relatively rigid CH=N bond. In contrast, hydrogenation of CH=N to CH₂–NH as expected, would increase N basicity and make the conformation of the metal complex more flexible and hence resulting in active sites without severe blockage of the channels in zeolitic matrix [16]. Most importantly, the hydrogenated ligands are more robust towards leaching than their Schiff base counterparts, due to immunity from the CH=N break in the case of acidic conditions, as indirectly revealed by the pioneering works of Luo [17], Baleizão [18] and Sheldon [19]. Recently, the catalytic performances of supported metal tetrahydro-salen complexes have drawn a lot of attention due to their

¹ The article is published in the original.

capability to easily activate O_2 under very mild conditions. Cu(II), Co(II) and Fe(III) tetrahydro-salen complexes encapsulated in zeolite-Y have been reported to show improved catalytic activity in oxidation of cycloalkanes with H_2O_2 in comparison with the corresponding metal salen complexes [16]. Sakthivel and coworkers [20] grafted a Cu(II) tetrahydro-salen complex onto the iodasilane modified surfaces of MCM-41 and MCM-48 by a direct immobilization method, and the catalysts could be reused in epoxidation of cyclooctene without significant loss of reactivity. More recently, our group tethered Cu(II) and Co(II) tetrahydro-salen complexes onto amino-functionalized SBA-15, and these catalysts displayed enhanced activity for the aerobic oxidation of styrene compared to the their respective Cu(II) and Co(II) salen complexes [21].

Previously, we reported an oxovanadium(IV)-based hybrid heterogeneous catalyst system, in which a functionalized oxovanadium(IV) Schiff base complexes of type $[VO(N_2O_2)]$ bearing chloromethyl groups were synthesized, directly anchored onto amino-modified SBA-15 materials [22]. This material was highly active, selective to epoxide and truly heterogeneous for the liquid-phase oxidation of styrene with air as the oxidant.

As a continuation of this line of research, we firstly report here the encapsulation of dioxovanadium(V) complexes of tetrahydro-Schiff bases as well as Schiff bases into zeolite-Y by a flexible ligand method. These encapsulated metal complexes are fully characterized and screened as catalysts for the aerobic oxidation of styrene in presence of a sacrificial co-reductant isobutyralsaldehyde.

2. EXPERIMENTAL

2.1. Materials

The following chemicals were commercially available and were used as received: NaOH, ethylenediamine, 1,6-hexylenediamine, o-phenylenediamine, styrene (98%), $VOSO_4$, $VO(acac)_2$ and all organic solvents are A.R. grade. Salicylaldehyde (99%) is obtained from Acros Organics, New Jersey, USA.

2.2. Synthetic Procedures

2.2.1. Synthesis of neat dioxovanadium complexes.

First, Schiff base ligands were prepared and followed the procedures: 30 mmol of ethylenediamine, 1,6-hexylenediamine or o-phenylenediamine was dissolved in 20 mL of ethanol. The obtained solution was then slowly added to a solution composed of 60 mmol of salicylaldehyde and 40 mL of ethanol under stirring conditions. The resultant solution was further refluxed for 1 h, resulting in the precipitation of a yellow or orange solid, which was filtered and recrystallized from ethanol, and denoted respectively as $SalenH_2$,

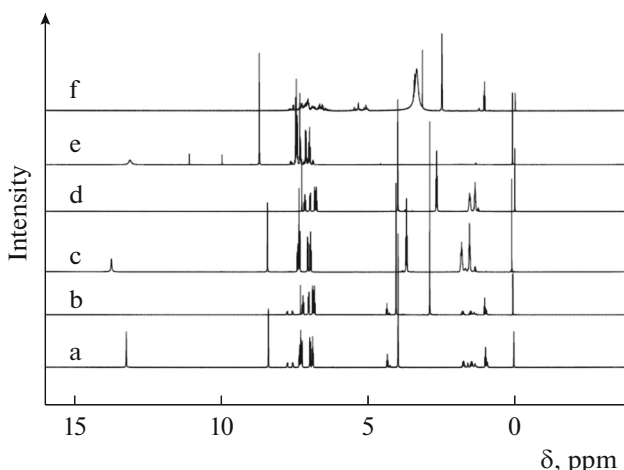


Fig. 1. 1H NMR spectra of (a) $SalenH_2$, (b) $[H_4]SalenH_2$, (c) $SalhexenH_2$, (d) $[H_4]SalhexenH_2$, (e) $SalphenH_2$ and (f) $[H_4]SalphenH_2$.

$SalhexenH_2$ and $SalphenH_2$. The 1H NMR spectra of $SalenH_2$, $SalhexenH_2$ and $SalphenH_2$ are shown in Fig. 1. 1H NMR ($CDCl_3$), δ , ppm: $SalenH_2$ – 13.20 (2H, s, OH), 8.35 (2H, s, CH=N), 7.30–6.82 (8H, m, Ar-H), 3.91 (4H, s, N- CH_2CH_2 -N) (Fig. 1a); $SalhexenH_2$ – 13.68 (2H, s, OH), 8.35 (2H, s, CH=N), 7.29–6.84 (8H, m, Ar-H), 3.62 (4H, t, N- $CH_2CH_2CH_2CH_2CH_2CH_2$ -N), 1.76–1.59 (4H, m, N- $CH_2CH_2CH_2CH_2CH_2CH_2$ -N), 1.38–1.22 (4H, m, N- $CH_2CH_2CH_2CH_2CH_2CH_2$ -N) (Fig. 1c); $SalphenH_2$ – 13.06 (2H, s, OH), 8.65 (2H, s, CH=N), 7.78–6.87 (12H, m, Ar-H) (Fig. 1e).

Schiff base ligand can be easily converted to tetrahydro-Schiff base ligand by the hydrogenation of $CH=N$ to CH_2-NH in presence of $NaBH_4$ in MeOH. Tetrahydro-Schiff base ligands were prepared as follows: 0.01 mol of $SalenH_2$, $SalhexenH_2$ or $SalphenH_2$ was dissolved in 60 mL of methanol, followed by the addition of 0.011 mol of $NaBH_4$ at ambient temperature. After stirring for 2 h, the solvent was removed under reduced pressure. The solid product was further washed with distilled water and recrystallized from ethanol, and the obtained materials were denoted as $[H_4]SalenH_2$, $[H_4]SalhexenH_2$ and $[H_4]SalphenH_2$, respectively. The 1H NMR spectra of $[H_4]SalenH_2$, $[H_4]SalhexenH_2$ and $[H_4]SalphenH_2$ are also shown in Fig. 1. 1H NMR ($CDCl_3$), δ , ppm: $[H_4]SalenH_2$ – 7.25–6.78 (8H, m, Ar-H), 3.99 (4H, s, N- CH_2CH_2 -N), 2.84 (4H, s, CH_2-NH) (Fig. 1b); $[H_4]SalhexenH_2$ – 7.18–6.69 (8H, m, Ar-H), 3.99 (4H, t, N- $CH_2CH_2CH_2CH_2CH_2CH_2$ -N), 1.56–1.49 (4H, m, N- $CH_2CH_2CH_2CH_2CH_2CH_2$ -N), 1.39–1.34 (4H, m, N- $CH_2CH_2CH_2CH_2CH_2CH_2$ -N), 2.69 (4H, s, CH_2-NH) (Fig. 1d); (DMSO- d_6), $[H_4]SalphenH_2$ –

7.58–6.61 (12H, m, Ar–H), 2.55 (4H, s, CH₂–NH) (Fig. 1f).

The procedures for the preparation of dioxovanadium(V) complexes of SalenH₂, SalhexenH₂, SalphenH₂ and [H₄]SalenH₂ were as follows: 2.0 mmol of Schiff base or tetrahydro-Schiff base ligand was dissolved in 20 mL of methanol, which was followed by the drop-wise addition of a solution of 2.0 mmol VO(acac)₂ in 10 mL of methanol at 65°C. The resultant solution was stirred and refluxed for 2 h. After cooling, the solid product was separated by filtration, and was further suspended in methanol and oxidized by passing air while stirring at room temperature for 24 h. The solid obtained was respectively denoted as VO₂-Salen, VO₂-Salhexen, VO₂-Salphen and VO₂-[H₄]SalenH₂. The procedures for the preparation of dioxovanadium(V) complexes of [H₄]SalhexenH₂ and [H₄]SalphenH₂ were as follows: 1.0 mmol of tetrahydro-Schiff base was mixed with 1.0 mmol of VO(acac)₂ in 6 mL of CH₂Cl₂, and the mixture was stirred at room temperature for 2 h. The resulting material was obtained by filtration, and further oxidized and denoted as VO₂-[H₄]Salhexen and VO₂-[H₄]Salphen.

2.2.2. Preparation of dioxovanadium-exchanged zeolite, VO₂-Y. Firstly, Na-Y was prepared according to the procedure reported with slight modification [23]. In a typical synthesis, 1.6 g of sodium hydroxide and 2.5 g of sodium aluminate (41 wt %) were dispersed in 25 mL of deionized water under constant stirring, and then 18 mL of silica sol (25 wt %) was added. The mixture with a molar composition of 13.2 SiO₂: 1.0 Al₂O₃: 16.4 Na₂O: 354 H₂O was stirred at room temperature for 1 h to form gel slurry, and then was hydrothermally crystallized at 100°C for 24 h. Subsequently, the resultant precipitate was separated from the mother liquor by filtration, washed with deionized water and dried at 150°C for 12 h.

Dioxovanadium-exchanged zeolite-Y (VO₂-Y) was prepared as follows: an amount of 8.0 g Na-Y zeolite was suspended in 240 mL of distilled water containing 9.48 mmol of VOSO₄. The mixture was stirred at 90°C for 24 h. The obtained materials were filtered, further oxidized by the procedure above, and washed with hot distilled water till the filtrate was free from any metal ion content and dried for 12 h at 150°C in air.

2.2.3. Preparation of encapsulated dioxovanadium(V) complexes, VO₂-L-Y (L = ligand). This process was performed with excess ligands ($n_{\text{ligand}}/n_{\text{metal}} = 3$), and allowed the insertion of ligand in the cavity of the zeolite followed by its complexation with metal ions. The complexation was carried out in MeOH at 80°C for 24 h. Uncomplexed ligands and the complexes adsorbed on the exterior surface were removed by full Soxhlet-extraction with MeOH till the eluate became colorless. The resulting sample was ion-exchanged with aqueous 0.01 M NaCl solution at 80°C for 8 h to

remove uncoordinated metal ions, followed by washing with deionized water until no Cl⁻ anions could be detected with AgNO₃ aqueous solution. The resulting VO₂-L-Y samples were dried at 150°C for several hours to constant weight. This procedure brought about brilliant color change, suggesting that the properties of neat compounds have been dramatically changed upon encapsulation.

2.3. Characterization

Powder XRD was collected with a Rigaku X-ray diffractometer with nickel filtered CuK_α radiation ($\lambda = 1.5418 \text{ \AA}$). The samples were scanned in the range $2\theta = 5\text{--}40^\circ$ and in steps of $4^\circ/\text{min}$. N₂ adsorption/desorption isotherms were recorded at -196°C with a Micromeritics ASAP 2020. Before measurements, the samples were outgassed at 120°C for 12 h. BET surface areas (S_{BET}) was calculated from adsorption branch in the relative pressure range from 0.05 to 0.30. The external surface area and pore volume were calculated by *t*-plot method. The infrared spectra (IR) of samples were recorded in KBr disks using a NICOLET impact 410 spectrometer (Melles Griot). UV-vis spectra were recorded on a Perkin Elmer UV-vis spectrophotometer Lambda 20 using barium sulfate as the standard in the range 200–800 nm. ¹H NMR experiments were carried out in sealed NMR tubes on a Varian Mercury-300 NMR spectrometer. Metal content was estimated by inductively coupled plasma atomic emission spectroscopy (ICPAES) analysis conducted on a Perkin Elmer emission spectrometer. Scanning electron microscopy (SEM) was performed on a JSM-6301F scanning microscope FEI instrument. The samples were coated with gold using a sputter coater. Total scattering patterns (Bragg and diffuse scattering data) were collected at the high energy beamline 11-ID-C at the Advanced Photo Source (APS) at Argonne National Laboratory, IL, USA. A wavelength of 0.10798 Å (115 keV) and 0.6 mm × 0.6 mm beam size were used to obtain two-dimensional (2D) diffraction patterns in transmission geometry using a Perkin-Elmer large area detector placed at 360 mm from the sample. Samples were packed into the Kapton capillaries, and the program Fit2D with a CeO₂ calibration standard was used to integrate the data. PDF patterns (G(*r*)) were obtained with the PDFGetX2 software and the data range used was up to 43 Å⁻¹. V K-edge XAFS spectra for the vanadium samples and a mixture of a reference compound and boron nitride which were pressed into self-supporting disks were measured at the 10-BM-B of Advanced Photo Source (APS) at Argonne National Laboratory. The X-ray absorption near edge structures (XANES) presented are fluorescence data and are average of at least two data sets from the same sample that were processed using standard pre-edge background subtraction and edge step normalization procedures.

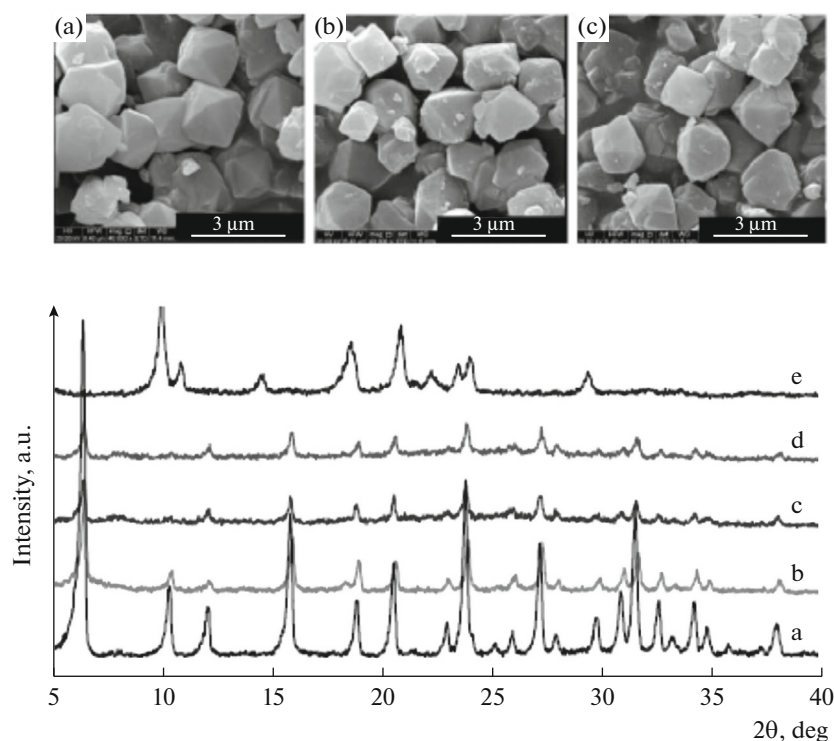


Fig. 2. XRD patterns of (a) Na-Y, (b) VO₂-Y, (c) VO₂-Salhexen-Y, (d) VO₂-[H₄]Salhexen-Y and (e) VO₂-Salhexen, and SEM images (inset) of (a) VO₂-Y, (b) VO₂-Salhexen-Y and (c) VO₂-[H₄]Salhexen-Y.

2.4. Catalytic Oxidation

The oxidation of styrene with air was carried out in a batch reactor. In a typical run, 10 mmol of styrene along with 10 mL of CH₃CN, 25 mmol of isobutyraldehyde and certain amount of catalyst were added into a 100 mL two-necked flask equipped with a condenser and an air pump. The reaction was started by bubbling the dry air with a stable flow rate of 80 mL min⁻¹ controlled by a flowmeter into the bottom of reactor at reaction temperature. After the reaction was finished, the catalyst was filtered, washed with CH₃CN, dried at 100°C overnight and reused directly without further purification. A leaching test was carried out by filtering the catalyst at the reaction temperature (80°C) after 1.5 h. At this time, half the volume was filtered and the resulting clear solution was allowed to react. The percentage of leaching was estimated by comparing the time-conversion plot of the twin reactions with and without solid. The liquid organic products were quantified by using a gas chromatography (Shimadzu, GC-8A) fitted with FID detector and HP-5 capillary column. The liquid organic products were identified by comparison with authentic samples and verified by GCMS coupling.

3. RESULTS AND DISCUSSION

3.1. Structural, Morphological and Textural Properties of Materials

The X-ray powder diffraction patterns of Na-Y, VO₂-Y and dioxovanadium complexes encapsulated in

zeolite-Y were recorded at 2θ values between 5° and 40° and are reproduced in Fig. 2. Compared to Na-Y, no remarkable difference, but only a small reduction in the intensity of peaks is observed, indicating that the zeolite framework has not undergone any significant structural change during the metal exchange and complex encapsulation processes [24], and thus the crystallinity of the zeolite is well preserved. No new peaks assigned to neat dioxovanadium complexes (Fig. 2e) can be detected in the encapsulated zeolites (Figs. 2c, 2d), indicating that the metal complexes encapsulated are highly dispersed in the zeolitic host [25]. The XRD patterns of other dioxovanadium complexes encapsulated in zeolite-Y are not shown here because their diffractograms are virtually the same and similar to that of VO₂-Salhexen-Y.

SEM micrographs of the modified zeolites exemplified by VO₂-Y, VO₂-Salhexen-Y and VO₂-[H₄]Salhexen-Y are depicted in the inset of Fig. 2 and show regular 2 μm cubic particles similarly to the parent material. The SEM images of VO₂-Salhexen-Y (Fig. 2b, inset) and VO₂-[H₄]Salhexen-Y (Fig. 2c, inset) show the presence of well-defined zeolite crystals free from any shadow of metal complexes present on their external surface, indicating that the crystallinity of parent zeolites was kept upon complex entrapment.

The nitrogen adsorption isotherms for the parent (Na-Y) and three representative modified zeolites are typical of microporous materials (not shown). Micropore volumes and external surface areas were calcu-

Table 1. Textual properties of various materials prepared

Materials	Microporous volume*, cm ³ /g	External surface are, m ² /g
Na-Y	0.320	17.7
VO ₂ -Y	0.258	38.4
VO ₂ -Salhexen-Y	0.170	92.7
VO ₂ -[H ₄]Salhexen-Y	0.210	85.4

* From the nitrogen adsorption isotherm at -196°C , calculated by the t -method.

lated by fitting the adsorption data in the corresponding theories; the values are given in Table 1. As expected, the micropore volumes of VO₂-Y and metal complex encapsulated zeolite-Y show an apparent reduction when compared with their respective parent materials. The lowering of the pore volumes indicate the presence of dioxovanadium complexes within the cavities of the zeolites, not on the external surface. Similar observation was also found for inclusion of Mn(III) Schiff base complexes into zeolite-Y [26]. On the other hand, the external surface areas determined from the t -plot increase with the incorporation of metal ions by comparing VO₂-Y with Na-Y. This increase can be explained in terms of the zeolite structural deformation occurring during the cation-exchanged process [27].

Varied information at atomic scale can be obtained by comparative study of pair distribution function (PDF) of samples at different preparation stages. As illustrated in Fig. 3, the PDFs of neat dioxovanadium complexes (Figs. 3f–3h) are quite different from those of zeolite based materials (Figs. 3a–3e), indicating the different interatomic distances present. However,

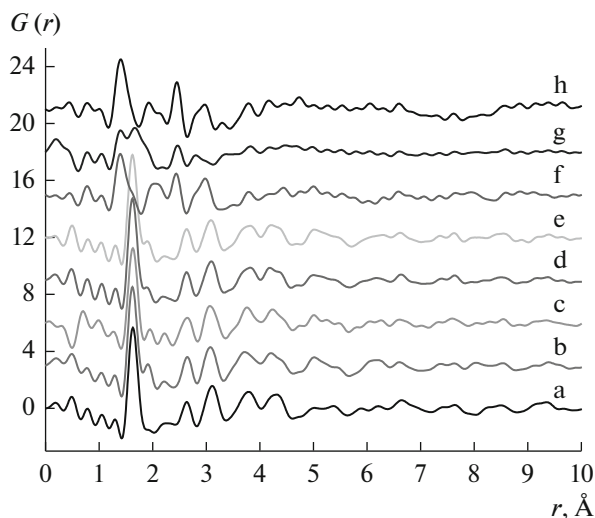


Fig. 3. Pair distribution functions for samples of (a) Na-Y, (b) VO₂-Y, (c) VO₂-[H₄]Salen-Y, (d) VO₂-[H₄]Salhexen-Y, (e) VO₂-Salhexen-Y, (f) VO₂-[H₄]Salen, (g) VO₂-[H₄]Salhexen and (h) VO₂-Salhexen.

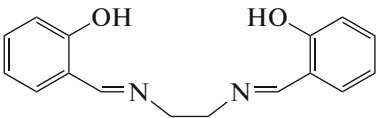
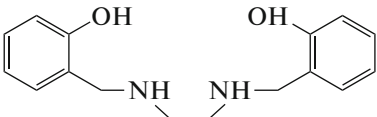
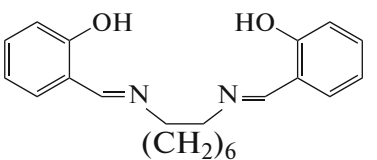
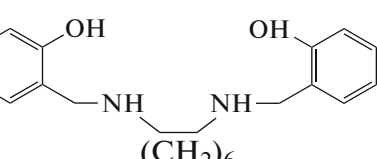
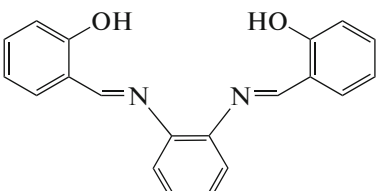
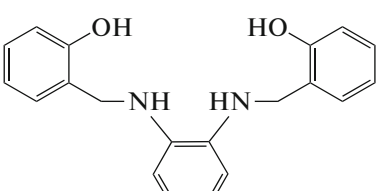
compared to Na-Y, all encapsulated vanadium complexes show nearly unchanged peaks in the region from 1.5 to 5 Å except for a small peak ca. 1.94 Å, and general intensity decrease consistent with a loss of long range order beyond 6 Å. The first strong peaks in the PDFs at ca. 1.63 Å, and the following weaker peaks ca. 2.64 Å are observed in all zeolite based materials, due to the overlapping T–O bonds within the (Si, Al)O₄ tetrahedra (T) [28], indicating the retention of the basic (Si, Al)O₄ tetrahedra building blocks with no measurable T–O bond breakage during the ion-exchange and encapsulation processes. The weak peaks at 1.94 Å in encapsulated samples are due to the V=O pairs [29], consistent with the peaks ranged from 1.8 to 2.2 Å for three neat dioxovanadium complexes, indicating that vanadium ions or vanadium complexes have been introduced into the supercages of zeolite.

3.2. Spectroscopic Characterization

¹H NMR spectra of all ligands show the aromatic protons as multiplet in the range 7.78–6.61 ppm (see Fig. 1 and Table 2). ¹H NMR spectra of three tetradentate Schiff base ligands of N₂O₂ donor sets possess two phenolic (13.06–13.68 ppm) and azomethine (8.35–8.65 ppm) groups [30]. The azomethine proton signals appearing in the spectra of Schiff base ligands are absent upon hydrogenation, indicating that CH=N moieties are completely converted to CH₂–NH groups through hydrogenation, which is in accordance with the newly present signals at 2.55–2.84 ppm due to NH–CH₂ protons in the spectra of tetrahydro-Schiff base ligands.

Figure 4 shows the IR spectra of various samples. The ligand SalhexenH₂ exhibits a band at 1646 cm⁻¹ due to azomethine ν_{C=N} stretch (Fig. 4a). This band registers a low frequency shift of ca. 29 cm⁻¹ in the spectra of VO₂-Salhexen (Fig. 4c), indicating the coordination of azomethine nitrogen to the vanadium [31]. However, the peak attributed to CH=N vibration disappears in the spectrum of [H₄]SalhexenH₂, and a new peak at 3288 cm⁻¹ attributed to N–H vibration is substitutionally observed upon hydrogenation (Fig. 4b). In the lower frequency region, the bands appeared at 985 and 1040 cm⁻¹ due to ν_{V=O} stretches in the spectra of VO₂-Salhexen and VO₂-[H₄]Salhexen are observed.

Table 2. Structure and ^1H NMR chemical shift of various ligands

Nomenclature	Structure	Chemical shift (ppm)				
		OH	CH=N	Ar-H	N(CH ₂) _x N	CH ₂ -NH
SalenH ₂		13.20	8.35	7.30–6.82	3.91	–
[H ₄]SalenH ₂		–	–	7.25–6.78	3.99	2.84
SalhexenH ₂		13.68	8.35	7.29–6.84	3.62, 1.76–1.59 1.38–1.22	–
[H ₄]SalhexenH ₂		–	–	7.18–6.69	3.99 1.56–1.49 1.39–1.34	2.69
SalphenH ₂		13.06	8.65	7.78–6.87	–	–
[H ₄]SalphenH ₂		–	–	7.58–6.61	–	2.55

Unfortunately, these bands could not be located upon complex encapsulation due to the appearance of strong and broad band of the zeolite framework in the $\sim 1000\text{ cm}^{-1}$ region. It is evident that framework vibration bands of zeolite-Y dominate the spectra below 1200 cm^{-1} for all samples. The bands at 462, 570, 699 and 784 as well as 1060 and 1122 cm^{-1} are attributed to T–O bending mode, double ring, symmetric stretching and asymmetric stretching vibrations, respectively [16]. No shift is observed upon introduction of metal ions and inclusion of metal complexes, further substantiating that the zeolite framework remains unchanged. In spite of this, there is obviously a difference in the range of $1200\text{--}1600\text{ cm}^{-1}$ and $550\text{--}450\text{ cm}^{-1}$ among zeolite-Y based samples. The bands

at $1200\text{--}1600\text{ cm}^{-1}$ in the spectra of $\text{VO}_2\text{-Salhexen-Y}$ (Fig. 4g) and $\text{VO}_2\text{-[H}_4\text{]Salhexen-Y}$ (Fig. 4h), assigned to C–O, C–N and aromatic ring vibrations of ligands, are absent in the case of Na-Y and $\text{VO}_2\text{-Y}$ samples. It is the same case with the bands at 536 and 513 cm^{-1} due to $\nu_{\text{V-O}}$ and $\nu_{\text{V-N}}$. All these data indicate that dioxovanadium complexes have been encapsulated inside zeolite-Y, and similar results can be obtained over other samples.

The UV-vis spectra of three representative samples for $[\text{H}_4]\text{SalhexenH}_2$, $\text{VO}_2\text{-[H}_4\text{]SalhexenH}_2$ and $\text{VO}_2\text{-[H}_4\text{]SalhexenH}_2\text{-Y}$ are reproduced in Fig. 5. The UV-vis spectrum of $[\text{H}_4]\text{SalhexenH}_2$ exhibits three bands at 337, 270 and 235 nm, assigned to $n\text{-}\pi^*$, $\pi\text{-}\pi^*$ and $\phi\text{-}\phi^*$ transitions, respectively. Appearance of these

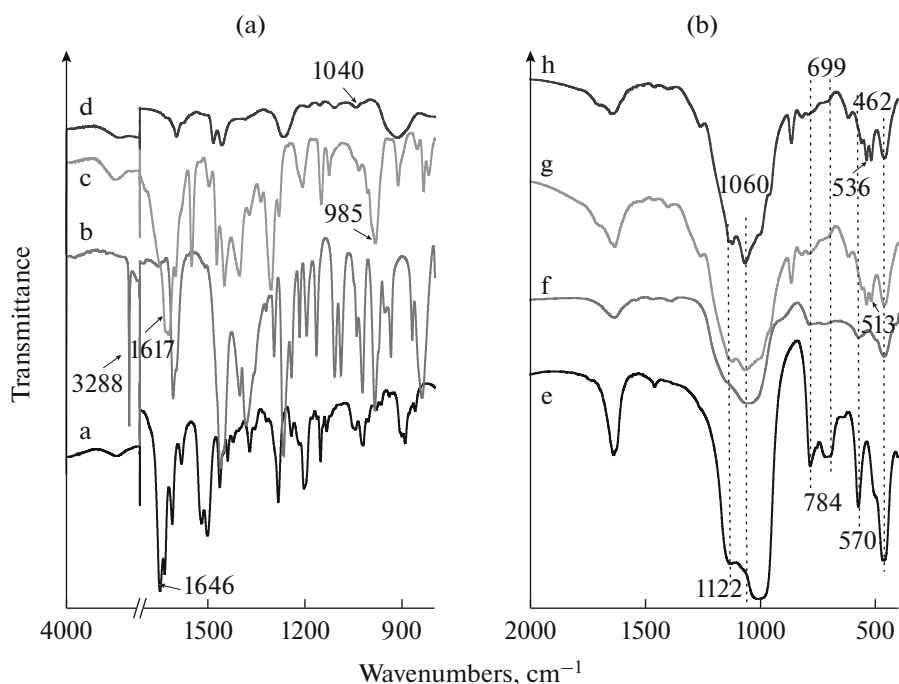


Fig. 4. FT-IR spectra of (a) SalhexenH₂, (b) [H₄]SalhexenH₂, (c) VO₂-Salhexen, (d) VO₂-[H₄]Salhexen, (e) Na-Y, (f) VO₂-Y, (g) VO₂-Salhexen-Y and (h) VO₂-[H₄]Salhexen-Y.

bands at lower energy values indicates the coordination of ligands to vanadium [32]. Additionally, all dioxovanadium complexes are dominated by the presence of several bands at 370–430 nm, assigned to ligand to metal charge transfer transition (LMCT) [16, 33].

Figure 6 shows different XANES spectra of various V-containing samples. The characteristics of the XANES spectra can be used as a fingerprint method to describe the V environment in a compound. A

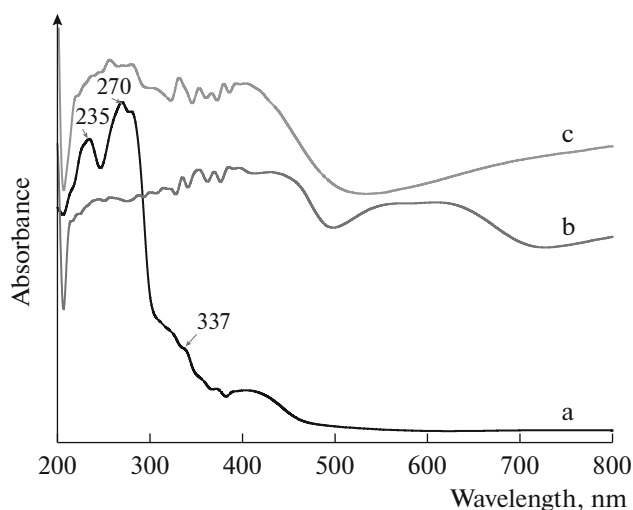


Fig. 5. UV-vis spectra of (a) SalhexenH₂, (b) VO₂-[H₄]Salhexen and (c) VO₂-[H₄]Salhexen-Y.

comparison among the spectra of the standards (VO, V₂O₃, VO₂ and V₂O₅) shows strong variations in energy position and intensity of peaks in the pre-edge region (before ca. 5480 eV) and the edge region (after 5480 eV). The increasing pre-edge intensity with increasing valence state was observed from V²⁺ to V⁵⁺ (see Figs. 6g–6j). The pre-edge peak is well-known to be due to a formally forbidden 1s → 3d electronic transition, which is dipole allowed if the full local O_h symmetry is decreased [34]. The pre-edge peak position and intensity ranged from 5469.4 to 5470.4 eV for VO₂-containing samples is near to that for standard V₂O₅ at 5468.2 eV, which indicates an oxidation state of V(5+) and the octahedral symmetry deviation for VO₂-containing samples. This also demonstrates that the recycled VO₂-[H₄]Salhexen-Y and VO₂-Salhexen-Y retain their oxidation state and distorted octahedral symmetry, as compared to their fresh ones. However, the pre-edge feature (mainly peak position) of neat dioxovanadium complexes is more close to V₂O₅ than their heterogeneous samples, indicating that zeolite matrix affects the V environment slightly.

3.4. Catalytic Properties

Table 3 summarizes the catalytic results (under optimized conditions) for the aerobic oxidation of styrene over various catalysts. The VO₂-Y catalyst is almost inactive for the oxidation of styrene (Entry 1), while VO₂-Schiff and VO₂-[H₄]Schiff base complexes

Table 3. Catalytic properties of various catalysts for the aerobic oxidation of styrene

Entry	Catalysts	V loading ^a , mmol/g	Styrene conversion ^b , %	TOF ^c , h ⁻¹	Product selectivity ^d (mol%)		
					Bza	So	others
1	VO ₂ -Y	0.9462	6.8	1.8	62.5	33.2	4.3
2	VO ₂ -[H ₄]Salen	2.9674	44.2	37.2	65.7	34.3	0
3	VO ₂ -[H ₄]Salhexen	2.5445	35.2	34.6	50.4	48.6	1.0
4	VO ₂ -[H ₄]Salphen	2.5974	50.6	48.7	40.2	45.6	14.2
5	VO ₂ -[H ₄]Salen-Y	0.2917	69.1	59.2	66.8	30.0	3.2
6	VO ₂ -[H ₄]Salhexen-Y	0.2688	95.2	88.5	57.6	42.4	0
7	VO ₂ -[H ₄]Salphen-Y	0.0703	65.1	231.5	24.6	30.8	44.6
8	VO ₂ -Salen	3.0030	96.2	80.1	50.0	35.6	14.4
9	VO ₂ -Salhexen	2.5707	51.4	50.0	66.4	33.6	0
10	VO ₂ -Salphen	2.6247	68.3	65.0	47.3	52.7	0
11	VO ₂ -Salen-Y	0.3568	44.1	30.9	59.4	29.5	11.1
12	VO ₂ -Salhexen-Y	0.4397	72.5	41.2	56.8	41.2	2.0
13	VO ₂ -Salphen-Y	0.1559	95.3	152.8	31.0	62.0	7.0
14	VO ₂ -[H ₄]Salhexen-Y (2nd)	—	95.0	—	55.7	44.3	0
15	VO ₂ -[H ₄]Salhexen-Y (3rd)	—	93.2	—	58.0	42.0	0
16	VO ₂ -[H ₄]Salhexen-Y (4th)	0.2620	90.6	86.4	54.2	45.8	0

^a Estimated by ICPAES. ^b Reaction conditions: supported catalyst 50.0 mg (5.0 mg for the neat catalyst), styrene 1.14 mL (10 mmol), CH₃CN 10 mL, flow of air 80 mL/min, isobutyraldehyde 2.28 mL (25 mmol), temperature 80°C and duration 8 h. ^c TOF, h⁻¹: (turn-over frequency) moles of substrate converted per mole metal ion per hour. ^d So: styrene oxide, Bza: benzaldehyde and others: including benzoic acid, phenylacetaldehyde and 1-phenylthane-1,2-diol.

and their encapsulated analogues in zeolite-Y exhibit activity, which substantiates that the active sites are dioxovanadium Schiff base or tetrahydro-Schiff base complexes, not metal ions. It is clear that the catalytic activities of encapsulated dioxovanadium complexes are always better over their respective non-encapsulated ones (see Entries 2–7, 9, 10, 12 and 13) except for VO₂-Salen-Y. These results suggest that encapsulation of neat metal complexes into zeolite-Y successfully isolated the neat complexes and prevented their dimerization. The enhanced activity of encapsulated catalyst may be also due to the synergistic beneficial catalytic interaction between the metal complexes and the zeolite support [35]. A leaching test for VO₂-Salhexen-Y and VO₂-[H₄]Salhexen-Y catalysts was performed to verify the heterogeneity of the catalytic process. In a duplicate reaction continued after removing the catalyst by filtration at reaction temperature, it was found that styrene could just be converted at a very low rate and this trend was almost parallel to the blank experiment (not shown). These results suggest that the large majority of the catalysis is carried out by a truly heterogeneous dioxovanadium catalyst. VO₂-Salhexen-Y and VO₂-[H₄]Salhexen-Y catalysts can be recycled three times without significant loss of activity and variation of their valence state.

Ligand hydrogenation affects catalytic properties significantly in our studies. VO₂-[H₄]Salen-Y catalyst shows higher activity than the corresponding VO₂-

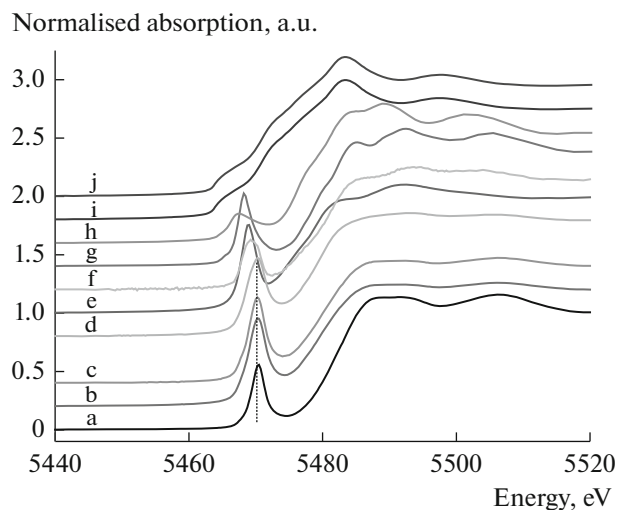


Fig. 6. Experimental V K-edge XANES spectra of (a) VO₂-Y, (b) VO₂-Salhexen-Y, (c) VO₂-[H₄]Salhexen-Y, (d) spent VO₂-[H₄]Salhexen-Y, (e) VO₂-Salhexen, (f) VO₂-[H₄]Salhexen, (g) V₂O₅, (h) VO₂, (i) V₂O₃ and (j) VO.

Salen-Y catalyst (Table 3, Entries 5 and 11). It is the same case with VO₂-[H₄]Salhexen-Y and VO₂-[H₄]Salphen-Y as compared to VO₂-Salhexen-Y and VO₂-Salphen-Y, respectively (Table 3, Entries 6, 7, 12 and 13), as revealed by the higher TOF values. These results demonstrated by our studies are consistent with the results reported in the literature [16, 36] that the improved Schiff base, i.e. tetrahydro-Schiff base ligands, are beneficial to the enhancement of catalytic activity. However, this conclusion seems to be false by comparison of neat dioxovanadium tetrahydro-Schiff base complexes with their respective dioxovanadium Schiff base complexes (Table 3, Entries 2–4 and 8–10), since activity decline was observed after hydrogenation of CH=N to CH₂-NH. According to literature [37], Schiff base ligands become more flexible after hydrogenation, resulting in easy formation of μ-oxo and μ-peroxo dimeric and other polymeric species especially when using oxidant, which may be responsible for the deficiency of neat tetrahydro-Schiff base complexes.

Additionally, we found that the acidic nature of hydrophilic zeolite was reflected in the product distribution in most conditions. The catalytic results over homogeneous complex catalysts show that benzaldehyde (Bza) is the major oxidation product, followed by styrene oxide (So), similar to literature [38, 39]. The encapsulated complexes show similar product distributions to the homogeneous counterparts, except for the presence of phenylacetaldehyde and 1-phenylethane-1,2-diol, formed via ring opening of phenyloxirane on acid sites. Lower styrene oxide selectivity for encapsulated catalysts is also connected with this ring opening reaction, suggesting that the acidity of the zeolite support declines the selectivity to phenyloxirane. However, the selectivity to styrene oxide was always higher than to benzaldehyde for VO₂-Salphen and VO₂-[H₄]Salphen whether encapsulated or not (Entries 4, 7, 10 and 13), which may be related to the great steric hindrance of dioxovanadium Salphen or [H₄]Salphen complexes.

CONCLUSIONS

Dioxovanadium(V) complexes of Schiff and tetrahydro-Schiff bases were successfully encapsulated in the supercages of zeolite-Y by a flexible ligand method, as evidenced by FT-IR, UV-vis spectroscopy, N₂ adsorption/desorption and XANES techniques. The structural integrity of zeolite throughout the encapsulation procedure was confirmed by XRD, SEM and PDF studies. These encapsulated metal complexes displayed better activity than their corresponding homogeneous analogues due to the site-isolation and synergism between dioxovanadium complexes and zeolite supports. All encapsulated dioxovanadium tetrahydro-Schiff base complexes show much higher activity in aerobic oxidation of styrene than

their corresponding Schiff base complexes due to the improved electronic environment around vanadium ions. Moreover, the selectivity to styrene oxide was lower than to benzaldehyde in most cases due to the acidic nature of zeolite matrix.

ACKNOWLEDGMENTS

This work and the use of Advanced Photon Source are supported by Office of Science, U.S. Department of Energy under Contract DE-AC02-06CH11357. Authors also thank J.T. Miller for the sharing standard vanadium sample data with us.

REFERENCES

1. Grigoropoulou, G., Clark, J.H., and Elings, J.A., *Green. Chem.*, 2003, vol. 5, p. 1.
2. Lane, B.S. and Burgess, K., *Chem. Rev.*, 2003, vol. 103, p. 2457.
3. Corma, A. and Garcia, H., *Chem. Rev.*, 2002, vol. 102, p. 3837.
4. Sato, T., Dakka, J., and Sheldon, R.A., *J. Chem. Soc., Chem. Commun.*, 1994, vol. 16, p. 1887.
5. Cambor, M.A., Corma, A., Martínez, A., and Pérez Parienta, J., *J. Chem. Soc., Chem. Commun.*, 1992, vol. 8, p. 589.
6. Tozzola, G., Mantegazza, M.A., Ranghino, G., Petrini, G., Bordiga, S., Ricchiardi, G., Lambertini, C., Zulian, R., and Zecchina, A., *J. Catal.*, 1998, vol. 179, p. 64.
7. Singh, A. and Selvam, T., *J. Mol. Catal. A: Chem.*, 1996, vol. 113, p. 489.
8. Sels, B.F., De Vos, D., and Jacobs, P.A., *Tetrahedron Lett.*, 1996, vol. 37, p. 8557.
9. Bansal, V.K., Thankachan, P.P., and Prasad, R., *Appl. Catal., A*, 2010, vol. 381, p. 8.
10. Sheldon, R.A., Arends, I.W.C.E., and Dijkman, A., *Catal. Today*, 2000, vol. 57, p. 157.
11. Balkus, K.J., Eissa, M., and Levado, R., *J. Am. Chem. Soc.*, 1995, vol. 117, p. 10753.
12. Canali, L. and Sherrington, D.C., *Chem. Soc. Rev.*, 1999, vol. 28, p. 85.
13. Kim, G.-J. and Shin, J.-H., *Catal. Lett.*, 1999, vol. 63, p. 83.
14. Katsuki, T., *Coord. Chem. Rev.*, 1995, vol. 140, p. 189.
15. O'Connor, K.J., Wey, S.J., and Burrows, C.J., *Tetrahedron Lett.*, 1992, vol. 33, p. 1001.
16. Jin, C., Fan, W.B., Jia, Y.J., Fan, B.B., Ma, J.H., and Li, R.F., *J. Mol. Catal. A: Chem.*, 2006, vol. 249, p. 23.
17. Luo, Y. and Lin, J., *Microporous Mesoporous Mater.*, 2005, vol. 86, p. 23.
18. Baleizao, C., Gigante, B., Das, D., Alvaro, M., Garcia, H., and Corma, A., *J. Catal.*, 2004, vol. 223, p. 106.
19. Sheldon, R.A., Arends, I.W.C.E., and Lempers, H.E.B., *Catal. Today*, 1998, vol. 41, p. 387.
20. Sakthivel, A., Sun, W., Raudaschl-Sieber, G., Chiang, A.S.T., Hanzlik, M., and Kühn, F.E., *Catal. Commun.*, 2006, vol. 7, p. 302.

21. Yang, Y., Zhang, Y., Hao, S.J., and Kan, Q.B., *Chem. Eng. J.*, 2011, vol. 171, p. 1356.
22. Yang, Y., Zhang, Y., Hao, S.J., Guan, J.Q., Ding, H., Shang, F.P., Qiu, P.P., and Kan, Q.B., *Appl. Catal. A: Gen.*, 2010, vol. 381, p. 274.
23. Htay, M.M., and Oo, M.M., *World Acad. Sci. Eng., Technol.*, 2008, vol. 48, p. 114.
24. Poltowicz, J., Pamin, K., Tabor, E., Haber, J., Adamski, A., and Sojka, Z., *Appl. Catal. A: Gen.*, 2006, vol. 299, p. 235.
25. Salavati-Niasari, M. and Amiri, A., *Appl. Catal. A: Gen.*, 2005, vol. 290, p. 46.
26. Salavati-Niasari, M., *Micropor. Mesopor. Mater.*, 2006, vol. 95, p. 248.
27. Sebastian, J., Mohan, K., and Jasra, R.V., *J. Catal.*, 2006, vol. 244, p. 208.
28. Readman, J.E., Forster, P.M., Chapman, K.W., Chupas, P.J., Parise, J.B., and Hriljac, J.A., *Chem. Commun.*, 2009, vol. 23, p. 3383.
29. Keller, D.E., Visser, T., Soulimani, F., Koningsberger, D.C., and Weckhuysen, B.M., *Vib. Spectrosc.*, 2007, vol. 43, p. 140.
30. Boghaei, D.M. and Mohebi, S., *J. Mol. Catal. A: Chem.*, 2002, vol. 179, p. 41.
31. Murphy, E.F., Schmid, L., Burgi, T., Maciejewski, M., and Baiker, A., *Chem. Mater.*, 2001, vol. 13, p. 1296.
32. Maurya, M.R., Chandrakar, A.K., and Chand, S., *J. Mol. Catal. A: Chem.*, 2007, vol. 270, p. 225.
33. Maurya, M.R., Kumar, A., Manikandan, P., and Chand, S., *Appl. Catal. A: Gen.*, 2004, vol. 277, p. 45.
34. Coulston, G.W., Bare, S.R., Kung, H., Birkeland, K., Bethke, G.K., Harlow, R., Herron, N., and Lee, P.L., *Science*, 1997, vol. 275, p. 191.
35. Gonzalez-Arellano, G., Corma, A., Iglesias, M., and Sanchez, F., *Inorg. Chim. Acta*, 2004, vol. 357, p. 3071.
36. Chen, P., Fan, B.B., Song, M.G., Jin, C., Ma, J.H., and Li, R.F., *Catal. Commun.*, 2006, vol. 7, p. 969.
37. Wang, X.L., Wu, G.D., Li, J.P., Zhao, N., Wei, W., and Sun, Y.H., *Catal. Lett.*, 2007, vol. 119, p. 87.
38. Indira, V., Halligudi, S.B., Gopinathan, S., and Gopinathan, C., *React. Kinet. Catal. Lett.*, 2001, vol. 73, p. 99.
39. Zsigmond, A., Horvath, A., and Notheisz, F., *J. Mol. Catal. A: Chem.*, 2001, vol. 171, p. 95.